

Effective dynamics for a spin-1/2 particle constrained to a curved layer with inhomogeneous thickness

Guo-Hua Liang(梁国华) and Pei-Lin Yin(尹佩林)

Citation: Chin. Phys. B, 2024, 33 (**2**): 020201. DOI: 10.1088/1674-1056/ad0715
Journal homepage: http://cpb.iphy.ac.cn; http://iopscience.iop.org/cpb

What follows is a list of articles you may be interested in

Enhanced mechanical and thermal properties of two-dimensional SiC and GeC with temperature and size dependence

Lei Huang(黄磊), Kai Ren(任凯), Huanping Zhang(张焕萍), and Huasong Qin(覃华松)
Chin. Phys. B, 2023, 32 (**7**): 076103. DOI: 10.1088/1674-1056/acc78f

Surface structure modification of $ReSe_2$ nanosheets via carbon ion irradiation

Mei Qiao(乔梅), Tie-Jun Wang(王铁军), Yong Liu(刘泳), Tao Liu(刘涛), Shan Liu(刘珊), and Shi-Cai Xu(许士才)
Chin. Phys. B, 2023, 32 (**2**): 026101. DOI: 10.1088/1674-1056/ac7297

Revealing Chern number from quantum metric

Anwei Zhang(张安伟)
Chin. Phys. B, 2022, 31 (**4**): 040201. DOI: 10.1088/1674-1056/ac2f2c

Finite-difference time-domain modeling of curved material interfaces by using boundary condition equations method

Jia Lu(卢佳), Huaichun Zhou(周怀春)
Chin. Phys. B, 2016, 25 (**9**): 090203. DOI: 10.1088/1674-1056/25/9/090203

Symmetry of Lagrangians of holonomic nonconservative system in event space

Zhang Bin(张斌), Fang Jian-Hui(方建会), and Zhang Wei-Wei(张伟伟)
Chin. Phys. B, 2012, 21 (**7**): 070208. DOI: 10.1088/1674-1056/21/7/070208

Effective dynamics for a spin-1/2 particle constrained to a curved layer with inhomogeneous thickness

Guo-Hua Liang(梁国华)† and Pei-Lin Yin(尹佩林)

School of Science, Nanjing University of Posts and Telecommunications, Nanjing 210023, *China*

(Received 15 August 2023; revised manuscript received 16 October 2023; accepted manuscript online 26 October 2023)

We derive an effective Hamiltonian for a spin-1/2 particle confined within a curved thin layer with non-uniform thickness using the confining potential approach. Our analysis reveals the presence of a pseudo-magnetic field and effective spin–orbit interaction (SOI) arising from the curvature, as well as an effective scalar potential resulting from variations in thickness. Importantly, we demonstrate that the physical effect of additional SOI from thickness fluctuations vanishes in low-dimensional systems, thus guaranteeing the robustness of spin interference measurements to thickness imperfection. Furthermore, we establish the applicability of the effective Hamiltonian in both symmetric and asymmetric confinement scenarios, which is crucial for its utilization in one-side etching systems.

Keywords: curved surface, inhomogeneous thickness, spin-1/2 particle, effective Hamiltonian

PACS: 02.40.–k, 61.46.–w, 61.72.–y, 68.65.–k **DOI:** 10.1088/1674-1056/ad0715

1. Introduction

Research of quantum motion in curved spacetime is a fundamental and captivating subject in physics, particularly when examining quantum phenomena occurring in the early universe and near black holes. Although astronomical observations provide valuable insights, experimental investigations on the effects of such large curvature are seemingly impossible. However, with advancements in micro and nanofabrication technology, laboratories are now able to manufacture nanostructures with various geometries.[1–5] Some of these low-dimensional nanostructures exhibit significant curvature, offering excellent platforms for studying the impact of curvature on quantum particles. With the aid of analog models, experiments involving different dynamics on a curved surface are expected to shed light on how space curvature influences the corresponding evolution processes. Optical experiments, for instance, have observed curvature effects on the correlation length of a beam,[6] the phase and group velocities of a wavepacket[7] and speckle patterns.[8] In the realm of quantum many-body systems, the observation of ultracold atomic bubbles[9] and Bose–Einstein condensate[10] in shell-shaped gases has been achieved.

Theoretically, the thin-layer procedure (TLP) was introduced as an appropriate method to describe the quantum dynamics on a curved surface.[11,12] This method naturally incorporates a scalar potential determined by the surface curvature in the effective two-dimensional (2D) equation, which is known as the geometric potential. Subsequently, the predicted potential was experimentally demonstrated in photonic crystals.[13] The geometric potential is attractive and leads to the formation of bound states, opening up new possibilities for constructing quantum dots[14,15] and quantum waveguides.[16–18] Inspired by these applications, numerous researchers have extended this method to other scenarios, including a charge particle in electric and magnetic fields,[19–21] a Dirac particle,[22–24] a spin-1/2 particle,[25–30] higher-dimensional induced gauge potential,[31–35] quantum scattering,[36] photons,[37–39] magnetism,[40,41] and quantum many-body systems.[42,43] It has been revealed that the effective dynamics exhibit additional geometric effects associated with the internal degrees of freedom and properties of the confined particle. Specifically, for spin-1/2 particles, the curvature induces pseudo-magnetic fields and effective spin–orbit interactions.

Most studies on the effective dynamics on curved surfaces have focused on motions within a thin layer of constant thickness, assuming that the ground state in the normal direction is independent of the surface coordinates. However, in reality, it is inevitable for low-dimensional structures to have an inhomogeneous thickness. Therefore, it is necessary to develop theoretical approaches that take into account the effect of varying thickness. In a previous work,[44] we extended TLP and derived the effective dynamics for a scalar particle confined to a curved surface with inhomogeneous thickness. It is found that the inhomogeneous confinement could induce an effective potential which is determined by the morphology of the thickness function, and is proportional to the ground state energy. This raises questions regarding spin-1/2 particles: Does the varying thickness induce additional spin–orbit interaction? Is the spin-dependent process affected by thickness fluctuations? Here, the extra spin–orbit interaction is supposed to be originated from the spin connection which can be viewed as an $SU(2)$ gauge field generated by local Lorentz

†Corresponding author. E-mail: lianggh@njupt.edu.cn

© 2024 Chinese Physical Society and IOP Publishing Ltd

transformation.[45] With this study we wish to clarify the problems and give the explicit Hamiltonian for a spin-1/2 particle constrained to a curved surface with inhomogeneous thickness.

The article is organized as follows. In Section 2, we derive the effective Hamiltonian for a spin-1/2 particle constrained to an arbitrary curved surface by an inhomogeneous confinement. Then we discuss the case of asymmetric confining potential in Section 3 and summarize our result in Section 4.

2. Effective dynamics

A curved surface $\mathcal{S}$ in three-dimensional (3D) Euclidean space can be described by a position vector $\boldsymbol{r}(q_1,q_2)$, where (q_1,q_2) are the curvilinear coordinates, as illustrated in Fig. 1. We assume that a spin-1/2 particle is bounded to a thin layer with varying thickness by a confining potential V_c. The thickness of the layer is symmetric about $\mathcal{S}$. Considering the inhomogeneity of the thickness, we use the adapted coordinate system (q_1,q_2,Q_3) to parameterize the portion of space near $\mathcal{S}$,

$$\boldsymbol{R}(q_1,q_2,Q_3)=\boldsymbol{r}(q_1,q_2)+\frac{Q_3}{\sqrt{s(q_1,q_2)}}\hat{N}(q_1,q_2), \quad (1)$$

where $\hat{N}$ is the unit vector normal to the surface, and $|Q_3|/\sqrt{s(q_1,q_2)}$ gives the distance from $\mathcal{S}$. Here, $s(q_1,q_2)$ is a dimensionless and continuous function close to unity, which determines the morphology of thickness. We expect this parametrization to absorb the inhomogeneity of thickness and facilitate the separation of dynamics perpendicular and tangent to the surface.

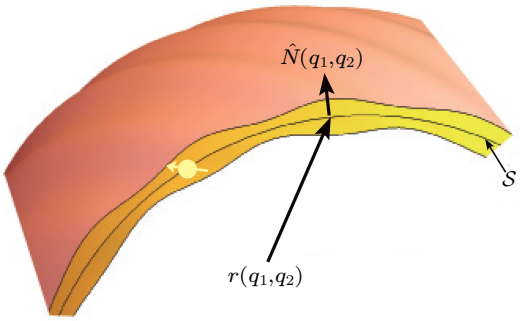


Fig. 1. Schematic diagram of a curved thin-layer with inhomogeneous thickness. Surface $\mathcal{S}$ is in the middle of the layer. A spin-1/2 particle is confined to the layer (yellow region).

To constrain the particle to $\mathcal{S}$, the confining potential V_c should have a deep minimum at the surface ($Q_3=0$), thus being expanded as a power series in Q_3,

$$V_c(Q_3)=\frac{m}{2}\omega^2(Q_3/\sqrt{s})^2+O[(Q_3)^3], \quad (2)$$

where m is the particle mass and $\omega=\omega_0 s(q_1,q_2)$, wherein ω_0 is a constant intensity parameter. In quantum mechanics, as a harmonic oscillator potential, the leading term of V_c corresponds to a region with width $d\propto 1/\sqrt{\omega}$, within which the particle is found with high probability. Therefore, it is reasonable to define d as the thickness of the thin-layer around $\mathcal{S}$, which is proportional to $1/\sqrt{s}$.

We can straightforwardly obtain

$$\begin{aligned}\partial_a\boldsymbol{R}&=\partial_a\boldsymbol{r}+\frac{Q_3}{\sqrt{s}}(\partial_a\hat{N})+\mathcal{A}_aQ_3\hat{N},\\ \partial_3\boldsymbol{R}&=\frac{1}{\sqrt{s}}\hat{N},\end{aligned} \quad (3)$$

where $\mathcal{A}_a=\partial_a(1/\sqrt{s})$ and the index $a=1,2$ (so does b,c in the text below). The derivatives of the normal vector $\hat{N}(q_1,q_2)$ can be expressed by the tangent vectors of the surface,

$$\partial_a\hat{N}=\alpha_{ab}\partial_b\boldsymbol{r}, \quad (4)$$

where α_{ab} is called the Weingarten curvature matrix. Thus, the parametrization (1) leads to the covariant components of the three-dimensional metric tensor via $G_{AB}=\partial_A\boldsymbol{R}\cdot\partial_B\boldsymbol{R}$ with $A,B=1,2,3$. The metric can be split into two parts

$$G_{AB}=\tilde{G}_{AB}+K_{AB}, \quad (5)$$

where

$$\tilde{G}_{AB}=\begin{pmatrix}\gamma_{ab} & \boldsymbol{0}\\ \boldsymbol{0} & 1\end{pmatrix}, \quad (6)$$

$$K_{AB}=\begin{pmatrix}Q_3^2\mathcal{A}_a\mathcal{A}_b & Q_3\mathcal{A}_a/\sqrt{s}\\ Q_3\mathcal{A}_b/\sqrt{s} & 1/s-1\end{pmatrix}, \quad (7)$$

with

$$\gamma_{ab}=g_{ab}+\frac{Q_3}{\sqrt{s}}[\alpha g+(\alpha g)^{\mathrm{T}}]_{ab}+\frac{Q_3^2}{s}(\alpha g\alpha)_{ab}, \quad (8)$$

and $g_{ab}=\partial_a\boldsymbol{r}\cdot\partial_b\boldsymbol{r}$ is the 2D metric tensor for the surface $\mathcal{S}$. Here, $\tilde{G}_{AB}$ corresponds to the case of constant thickness, while K_{AB} is obviously originated from the thickness fluctuation. The determinant of G_{AB} is found to be $G=|\gamma|/s$.

It is also necessary to deduce the exact form of the inverse of the metric tensor, which turns out to be

$$G^{AB}=\begin{pmatrix}\lambda^{ab} & -\lambda^{ac}Q_3\sqrt{s}\mathcal{A}_c\\ -\lambda^{bc}Q_3\sqrt{s}\mathcal{A}_c & s(1+Q_3^2\mathcal{A}_c\lambda^{cd}\mathcal{A}_d)\end{pmatrix}, \quad (9)$$

where $\lambda^{ab}=(\gamma_{ab})^{-1}$ is the inverse of γ_{ab}.

Before considering the dynamic equation, we need introduce the dreibeins E_A^I for the 3D metric, which satisfy the relation $G_{AB}=E_A^IE_B^J\delta_{IJ}$ (δ_{IJ} is a unit matrix and $I,J=1,2,3$ refer to the local flat indices). According to the structure of G_{AB}, we choose the dreibeins to be

$$E_a{}^3=Q_3\mathcal{A}_a,\ \ E_3{}^3=1/\sqrt{s},\ \ E_3{}^i=0, \quad (10)$$

and other components satisfy $\gamma_{ab}=E_a{}^iE_b{}^j\delta_{ij}$ ($i,j=1,2$). The form of $E_a{}^i$ is the same as the terms of constant thickness case in Ref. [30], which is

$$E_a{}^i=e_a{}^i+(Q_3/\sqrt{s})\alpha_a^be_b{}^i, \quad (11)$$

where e_a^i are the veilbeins for the 2D metric g_{ab}, namely $g_{ab} = e_a^i e_b^j \delta_{ij}$.

The 3D Hamiltonian for a non-relativistic spin-1/2 particle moving in a curved space with the confining potential V_c is of the form

$$H_{3D} = -\frac{\hbar^2}{2m}\Big[\frac{1}{\sqrt{G}} D_A(\sqrt{G}G^{AB}D_B) - \frac{1}{4}\bar{R}\Big] + V_c(Q_3). \quad (12)$$

where $\bar{R}$ is the Ricci scalar (which will be neglected in the following as it vanishes when $Q_3 \to 0$) and D_A is a gauge invariant derivative, $D_A = \partial_A + \bar{\Omega}_A$, with the spin connection

$$\bar{\Omega}_A = \frac{\mathrm{i}}{4}\bar{\omega}_{AIJ}\varepsilon^{IJK}\sigma_K, \quad (13)$$

$$\bar{\omega}_{AIJ} = E_I^B(\partial_A E_{BJ} - \bar{\Gamma}_{AB}^C E_{CJ}), \quad (14)$$

where ε^{IJK} is the Levi–Civita symbol and σ_K are Pauli matrices. To distinguish the geometric quantities in 3D and 2D space, we mark the ones in 3D space with bars. For example, the Christoffel symbols $\bar{\Gamma}_{AB}^C = G^{CD}(\partial_B G_{DA} + \partial_A G_{DB} - \partial_D G_{AB})/2$, while $\Gamma_{ab}^c = g^{cd}(\partial_b g_{da} + \partial_a g_{db} - \partial_d g_{ab})/2$.

After some calculations (the calculation details are presented in Appendix), the tangential components of the spin connection are obtained,

$$\bar{\Omega}_a = \Omega_a + \mathrm{i}(A_{so})_a + O(Q_3), \quad (15)$$

where $\Omega_a = \frac{\mathrm{i}}{4}\varepsilon^{ij}\omega_{aij}\sigma_3$, and $(A_{so})_a = \frac{1}{2\sqrt{g}}\varepsilon^{bc}\sigma_b\alpha_{ac}$. It is found that the expression of tangential components are the same as the case of constant thickness, consisting of two main parts: Ω_a leads to the pseudo-magnetic field and A_{so} gives the effective spin–orbit interaction. However, the normal component is

$$\bar{\Omega}_3 = \frac{\mathrm{i}}{2}Q_3\frac{\mathcal{A}_c}{\sqrt{s}}\varepsilon^{ab}\alpha_b^c\sigma_a + O(Q_3^2), \quad (16)$$

which gives a non-vanishing term up to the first order in Q_3, compared with the constant thickness case.

The corresponding wavefunction Φ for H_{3D} satisfies the normalization condition

$$\int |\Phi|^2\sqrt{G}\,\mathrm{d}q_1\,\mathrm{d}q_2\,\mathrm{d}Q_3 = 1. \quad (17)$$

We are aiming at obtaining an effective Hamiltonian whose wavefunction describes the quantum probability density on the 2D surface S. Hence it is necessary to rescale Φ by $(|G|/|g|)^{1/4}$, namely $\Psi = (|G|/|g|)^{1/4}\Phi$. The normalization of the new wavefunction Ψ is then

$$\int |\Psi|^2\,\mathrm{d}Q_3\sqrt{g}\,\mathrm{d}q_1\,\mathrm{d}q_2 = 1. \quad (18)$$

It is clear that we can now view $\int|\Psi|^2\mathrm{d}Q_3$ as a probability density for a particle moving on $\mathcal{S}$ with the curvilinear measure $\sqrt{g}\,\mathrm{d}q_1\,\mathrm{d}q_2$. The Hamiltonian should correspondingly be rescaled as $H = (|G|/|g|)^{1/4}H_{3D}(|G|/|g|)^{-1/4}$. By introducing operators $\hat{D}_a = D_a - \mathcal{A}_a\sqrt{s}Q_3\partial_3$, the rescaled Hamiltonian can be written in a compact form

$$H = -\frac{\hbar^2}{2m}\Big[sG^{-\frac{1}{4}}D_3\sqrt{G}D_3G^{-\frac{1}{4}} + (gG)^{-\frac{1}{4}}\hat{D}_a\sqrt{G}\lambda^{ab}\hat{D}_b(g/G)^{\frac{1}{4}}\Big] + V_c(Q_3). \quad (19)$$

To evaluate the intensity of V_c, we introduce a small and dimensionless parameter ε and rescale the harmonic frequency as $\omega \to \omega/\varepsilon$. Through adjusting ε, the harmonic binding could be large enough to limit the particle to the vicinity of $Q_3 = 0$. Therefore, ε can be an indicator of different energy scales and also serve as a perturbative parameter if we rescale the normal coordinate as $Q_3 \to \sqrt{\varepsilon}Q_3$. In this way, turning to Eq. (2) and neglecting the terms of order $(Q_3)^3$ and higher, we can find that V_c is of the order ε^{-1}. The Hamiltonian (19) can be written in powers of ε as

$$H = \varepsilon^{-1}(H_0) + \varepsilon^0(H_1 + H_1') + O(\varepsilon^{1/2}), \quad (20)$$

where

$$H_0 = s\Big[-\frac{\hbar^2}{2m}\partial_3^2 + \frac{m}{2}\omega_0{}^2(Q_3)^2\Big], \quad (21)$$

$$H_1 = -\frac{\hbar^2}{2m}s^{-\frac{1}{4}}\Big[\frac{1}{\sqrt{g}}\hat{D}_a(\sqrt{g}g^{ab}\hat{D}_b)\Big]s^{\frac{1}{4}} + V_g, \quad (22)$$

$$H_1' = -\frac{s\hbar^2}{2m}[2\bar{\Omega}_3\partial_3 + (\partial_3\bar{\Omega}_3)]. \quad (23)$$

Here, $V_g = -\frac{\hbar^2}{2m}(M^2 - K)$ is the well-known geometric potential, with the mean curvature $M = \mathrm{Tr}(\alpha_{ab})/2$ and Gaussian curvature $K = \det(\alpha_{ab})$. During the calculation, we have used the fact that $\sqrt{|\gamma|} = [1 + \mathrm{Tr}(\alpha_{ab})Q_3/\sqrt{s} + \det(\alpha_{ab})(Q_3)^2/s]\sqrt{|g|}$. Containing $\bar{\Omega}_3$, H_1' is expected to contribute extra spin–orbit interaction originated from the thickness variation.

In Eq. (20), H_0 describes a particle bounded by the harmonic oscillator potential in the transverse direction and takes a lead role in H, while $H_1 + H_1'$ seemingly gives the quantum dynamics in the tangential direction on $\mathcal{S}$. Specifically, H_1' arises from the variation in thickness, a term not observed in the case of constant thickness. To get the effective 2D Hamiltonian we must separate the wavefunction in the Schrödinger equation $H\Psi = E\Psi$, where E denotes the total energy. In this paper, we focus on the energy range where the state in the normal direction is always the ground state. Making the ansatz $\Psi = \sum_\beta u_\beta(q_1, q_2)\chi_\beta(Q_3)$, where β labels the spin degeneracy for H_0, we obtain

$$\Big[-\frac{\hbar^2}{2m}\partial_3^2 + \frac{m}{2}\omega_0^2(Q_3)^2\Big]\chi_\beta = \varepsilon E_0\chi_\beta, \quad (24)$$

$$[H_1 + H_1' + (s-1)E_0]u_\beta = E_1 u_\beta, \quad (25)$$

where $E_1 = E - E_0$. Note that E_0 in Eq. (24) is of the order $1/\varepsilon$, which is supposed to be the ground state energy and also the dominant part of the total energy E. Equation (25) describes the 2D effective dynamics on $\mathcal{S}$ under the transverse

mode energy E_0. Taking into account $E_0 \sim \varepsilon^{-1}$ in Eq. (25), we must keep $(s-1) \sim \varepsilon$, which gives the application range of our method.

As the spin degeneracy, the effective 2D Hamiltonian should be a 2×2 matrix, with the elements

$$\mathcal{H}_{\beta\beta'} = \int \chi_\beta^* [H_1 + H_1' + (s-1)E_0]\chi_{\beta'}\,\mathrm{d}Q_3. \tag{26}$$

To calculate this integral, one needs to utilize $\int \chi_\beta^* Q_3 \partial_3 \chi_{\beta'}\,\mathrm{d}Q_3 = -\frac{1}{2}\delta_{\beta\beta'}$. This equality leads to the conclusion

$$\int \chi_\beta^* H_1' \chi_{\beta'}\,\mathrm{d}Q_3 = 0, \tag{27}$$

indicating that, to the order of ε^0, the thickness variation of curved thin-layer does not give rise to an extra spin–orbit interaction in the 2D effective Hamiltonian. It should be noted that, although no physical effect exhibits from the 2D information, the combination of curvature and thickness gradient does result in a non-zero spin connection component $\bar{\Omega}_3$, which may affect the spin density distribution in the direction of thickness.

Performing the integral in Eq. (26) we eventually find that the effective Hamiltonian matrix is diagonal and the explicit form is

$$\mathcal{H}_{\text{eff}} = -\frac{\hbar^2}{2m}\frac{1}{\sqrt{g}} D_a(\sqrt{g}g^{ab}D_b) + V_{\text{g}} + (s-1)E_0. \tag{28}$$

In this effective Hamiltonian, V_{g} and $(s-1)E_0$ are two scalar potentials, which are due to the surface curvature and the thickness variation, respectively. Compared to the geometric potential V_{g}, the effective potential $(s-1)E_0$ depends on the ground state energy in the normal direction of the surface. It has been clarified that $\bar{\Omega}_a$ contained in the gauge derivative is composed of Ω_a and A_{so}, which lead to the pseudo-magnetic field with intensity K and the effective spin–orbit interaction with coupling tensor determined by the Weingarten matrix.

A key conclusion we draw here is that the thickness variation of the curved thin-layer does not bring an extra spin–orbit interaction in the effective dynamics. The reason for this is that obtaining the 2D tangential dynamics requires freezing and integrating the state perpendicular to the surface, which inherently neutralizes the detailed information in the thickness direction. This conclusion suggests that, despite the scalar potential $(s-1)E_0$, the energy splitting dependent on spin remains unaffected by thickness imperfection in thin-layer systems with arbitrary geometries, highlighting the reliability of spin interference measurements in relevant experiments.

3. Asymmetric confinement

The effective Hamiltonian (28) is obtained under the condition of symmetric confinement in the normal direction, namely $V_{\text{c}}(Q_3)$ is an even function. In reality, many 2D systems are under the confining potential with inversion asymmetry. In the following, we study the case of asymmetric confinement to figure out whether the Hamiltonian (28) is still applicable. The system to be considered is shown in Fig. 2(a), with the modification that one of the layer side is a hard-wall potential [see Fig. 2(b)], which could totally reflect the wave function. The corresponding confining potential can be expressed as

$$\tilde{V}_{\text{c}}(Q_3) = \begin{cases} \infty, & Q_3 < 0, \\ V_{\text{c}}(Q_3), & Q_3 \geq 0. \end{cases} \tag{29}$$

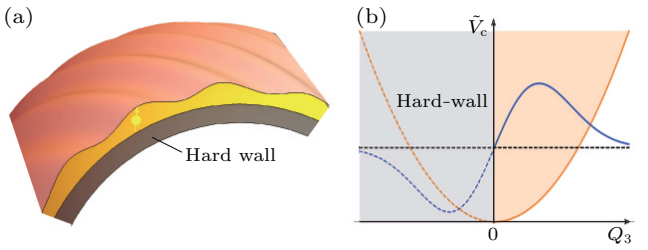


Fig. 2. (a) Schematic picture of a curved thin-layer with asymmetric confinement. One side is the same as Fig. 1 and the other side is a hard-wall potential. (b) The confining potential and bound state as a function of Q_3. The dashed lines correspond to the symmetric confinement.

The Hamiltonian (20) still holds in this condition after replacing the confining potential in Eq. (21). As before, we make the assumption $\Psi = \sum_\beta u_\beta(q_1,q_2)\bar{\chi}_\beta(Q_3)$, where $\bar{\chi}$ (here we ignore the degenerate index) satisfies the 1D equation

$$\left[-\frac{\hbar^2}{2m}\partial_3^2 + \tilde{V}_{\text{c}}/s\right]\bar{\chi} = \varepsilon E_0 \bar{\chi}. \tag{30}$$

It is obvious that putting together the new confining potential $\tilde{V}_{\text{c}}(Q_3)$ in $Q_3 > 0$ and its mirror image $\tilde{V}_{\text{c}}(-Q_3)$ in $Q_3 < 0$ recovers the harmonic oscillating potential V_{c}. Considering the boundary condition, all the odd eigenfunctions χ which vanish at $Q_3 = 0$ satisfy Eq. (30) in the range $Q_3 > 0$. Taking into account the normalization, the ground state $\bar{\chi}^{(0)} = \sqrt{2}\chi^{(1)}$, with $\chi^{(1)}$ the first excited state in symmetric case. One can easily confirm the equality $\int_0^\infty \bar{\chi}^{(0)*} Q_3 \partial_3 \bar{\chi}^{(0)}\,\mathrm{d}Q_3 = -\frac{1}{2}\delta_{\beta\beta'}$, which makes the integral of H_1' vanish again. Likewise, replacing χ with $\bar{\chi}$ and performing the integral of H, we can obtain the same effective Hamiltonian. Therefore, for the thin-layer system with asymmetric confinement, $\mathcal{H}_{\text{eff}}$ is still applicable.

4. Conclusion

In conclusion, we obtain an effective Hamiltonian for a spin-1/2 particle constrained to an arbitrary curved thin layer with varying thickness by using the confining potential approach. It is shown that the pseudo-magnetic field and effective spin–orbit interaction of constant thickness case are still applicable and thickness variation does not lead to an extra spin–orbit interaction. This result implies a robustness of spin-dependent energy splitting to the thickness fluctuations

in curved thin-layer systems. Our result is also proved to be valid for both symmetric and asymmetric confinement cases. The latter can be utilized to describe one-side etching structures, which are more common in fabrication of waveguides and metamaterials. By providing a theoretical tool, this effective Hamiltonian allows for a quick assessment of the geometric effects on properties of low-dimensional nanostructures and aids in design processes.

Appendix A: Calculation details in the separation of dynamics

In differential geometry, the dreibein $E_A^{\ I}$ is a set of orthogonal space vector fields that diagonalize the metric tensor, $G_{AB}=E_A^{\ I}E_B^{\ J}\delta_{IJ}$. The conbein $E_I^{\ A}$ satisfies $E_A^{\ I}E_I^{\ B}=\delta_A^B$ and $E_A^{\ I}E_J^{\ A}=\delta_J^I$. Accordingly, the inverse of the dreibein in this paper is found to be

$$\begin{aligned}
&E_i^{\ a}=(E_a^{\ i})^{-1},\ \ E_3^{\ 3}=\sqrt{s},\\
&E_1^{\ 3}=\frac{\sqrt{s}Q_3}{|E_a^{\ i}|}[E_1^{\ 2}\mathcal{A}_2-E_2^{\ 2}\mathcal{A}_1],\\
&E_2^{\ 3}=\frac{\sqrt{s}Q_3}{|E_a^{\ i}|}[E_2^{\ 1}\mathcal{A}_1-E_1^{\ 1}\mathcal{A}_2].
\end{aligned}\tag{A1}$$

To calculate the spin connection, we need give the explicit form of the geometric quantities up to the first or second order of Q_3 (which depends on whether the term contains derivative to Q_3). For the Christoffel symbols, we can find

$$\begin{aligned}
\bar{\Gamma}_{ab}^{c}=&\Gamma_{ab}^{c}+O(Q_3),\\
\bar{\Gamma}_{ab}^{3}=&-\bar{\Gamma}_{ab}^{c}\mathcal{A}_c\sqrt{s}Q_3+\frac{s}{2}(G_{3a,b}+G_{3b,a}-G_{ab,3})+O(Q_3^2)\\
=&-\Gamma_{ab}^{c}\mathcal{A}_c\sqrt{s}Q_3+\frac{s}{2}\Big[2G_{3a,b}-\frac{2\alpha_{ab}}{\sqrt{s}}-\frac{2Q_3(\alpha g\alpha)_{ab}}{s}\\
&-2Q_3\mathcal{A}_a\mathcal{A}_b\Big]+O(Q_3^2)\\
=&-\alpha_{ab}\sqrt{s}+Q_3[-\Gamma_{ab}^{c}\mathcal{A}_c\sqrt{s}+\sqrt{s}\partial_a\mathcal{A}_b-(\alpha g\alpha)_{ab}]\\
&+O(Q_3^2),\\
\bar{\Gamma}_{3a}^{b}=&\bar{\Gamma}_{a3}^{b}=\frac{1}{2}G^{bc}\partial_3G_{ac}+\frac{1}{2}G^{b3}\partial_aG_{33},\\
\bar{\Gamma}_{3a}^{3}=&\frac{1}{2}G^{3b}\partial_3G_{ab},\\
\bar{\Gamma}_{33}^{A}=&0.
\end{aligned}\tag{A2}$$

Next we are able to calculate the spin connection terms,

$$\begin{aligned}
&\bar{\omega}_{aij}=\omega_{aij}+O(Q_3),\\
&\bar{\omega}_{a3j}=-\frac{\sqrt{s}}{2}E^{c}_{\ j}\partial_3G_{ac}+O(Q_3)=-\alpha_{ac}E^{c}_{\ j}+O(Q_3),\\
&\bar{\omega}_{ai3}=-\bar{\omega}_{a3i}=\alpha_{ac}E^{c}_{\ i},
\end{aligned}\tag{A3}$$

where $\omega_{aij}=e^b_{\ i}(\partial_ae_{bj}-\Gamma^c_{ab}e_{cj})$.

To calculate the normal component $\bar{\Omega}_3$, we must obtain

$$\begin{aligned}
\bar{\omega}_{3ij}=&E^b_{\ i}\Big[\alpha^a_be_{aj}-\Big(\frac{1}{2}E^a_{\ j}\partial_3G_{ba}+\frac{1}{2}E^3_{\ j}\partial_bG_{33}\Big)\Big]\\
=&e^b_{\ i}[-e^d_{\ j}Q_3\mathcal{A}_b\mathcal{A}_d-E^3_{\ j}\mathcal{A}_b/\sqrt{s}]+O(Q_3^2),
\end{aligned}\tag{A4}$$

$$\bar{\omega}_{3i3}=E^b_{\ i}\Big[-\frac{1}{2\sqrt{s}}G^{3a}\partial_3G_{ab}\Big].\tag{A5}$$

Therefore, we have

$$\begin{aligned}
\bar{\Omega}_3=&-\frac{\mathrm{i}}{4}Q_3e^b_{\ i}e^d_{\ j}\mathcal{A}_b\mathcal{A}_d\varepsilon^{ij3}\sigma_3+\frac{\mathrm{i}}{2}Q_3\frac{\mathcal{A}_c}{\sqrt{s}}e^b_{\ i}\alpha^c_b\varepsilon^{i3k}\sigma_k+O(Q_3^2)\\
=&-\frac{\mathrm{i}}{4}Q_3\varepsilon^{bd}\mathcal{A}_b\mathcal{A}_d\sigma_3+\frac{\mathrm{i}}{2}Q_3\frac{\mathcal{A}_c}{\sqrt{s}}\varepsilon^{ab}\alpha^c_b\sigma_a+O(Q_3^2)\\
=&\frac{\mathrm{i}}{2}Q_3\frac{\mathcal{A}_c}{\sqrt{s}}\varepsilon^{ab}\alpha^c_b\sigma_a+O(Q_3^2).
\end{aligned}\tag{A6}$$

The calculation details of $\bar{\Omega}_a$ can be seen in the appendix of Ref. [30]. To separate the dynamics in normal and tangential direction, the Laplacian can be written as

$$\begin{aligned}
&\frac{1}{\sqrt{G}}D_A(\sqrt{G}G^{AB}D_B)\\
=&\frac{1}{\sqrt{G}}D_3[\sqrt{G}(s+Q_3^2s^2\mathcal{A}_c\lambda^{cd}\mathcal{A}_d)D_3]\\
&+\frac{1}{\sqrt{G}}D_a(\sqrt{G}\lambda^{ab}D_b)-\frac{\sqrt{s}}{\sqrt{G}}D_a(\sqrt{G}\lambda^{ac}Q_3\mathcal{A}_cD_3)\\
&-\frac{\sqrt{s}}{\sqrt{G}}D_3(\sqrt{G}\lambda^{bc}Q_3\mathcal{A}_cD_b).
\end{aligned}\tag{A7}$$

By introducing operators $\hat{D}_a=D_a-\mathcal{A}_a\sqrt{s}Q_3\partial_3$, the third and fourth terms can be just integrated into the second term. That is why we have Eq. (19) in the main text.

Finally, H_1' can be calculated as

$$\begin{aligned}
H_1'=&-\frac{\hbar^2}{2m}s[G^{-1/4}\partial_3G^{1/4}\bar{\Omega}_3+G^{1/4}\bar{\Omega}_3\partial_3G^{-1/4}]\\
=&-\frac{\hbar^2}{2m}s[2\bar{\Omega}_3\partial_3+G^{-1/4}(\partial_3G^{1/4}\bar{\Omega}_3)+G^{1/4}\bar{\Omega}_3(\partial_3G^{-1/4})]\\
=&-\frac{\hbar^2}{2m}s[2\bar{\Omega}_3\partial_3+(\partial_3\bar{\Omega}_3)].
\end{aligned}\tag{A8}$$

It should be noted that the thickness variation function $s(q_1,q_2)$ results in no gauge potential in the effective Hamiltonian, despite the operator $\hat{D}_a$ including the term $\mathcal{A}_a\sqrt{s}Q_3\partial_3$. The reason is that the factor $s^{1/4}$ in Eq. (22) cancels out these terms in the integration of the effective Hamiltonian. This is expectable as the Hamiltonian needs to be Hermitian.

Acknowledgments

This work was supported in part by the National Natural Science Foundation of China (Grant No. 12104239), National Natural Science Foundation of Jiangsu Province of China (Grant No. BK20210581), Nanjing University of Posts and Telecommunications Science Foundation (Grant Nos. NY221024 and NY221100), the Science and Technology Program of Guangxi, China (Grant No. 2018AD19310), and the Jiangxi Provincial Natural Science Foundation (Grant No. 20224BAB211020).

References

[1] Ren Z and Gao P X 2014 *Nanoscale* **6** 9366
[2] Sun Q, Zhang R, Qiu J, Liu R and Xu W 2017 *Adv. Mater.* **30** 1705630
[3] Pogosov A G, Shevyrin A A, Pokhabov D A, Zhdanov E Y and Kumar S 2022 *J. Phys.: Condens. Matter* **34** 263001
[4] Lilian G, Laurent L, Guillaume L, Benoit W and Benjamin A 2022 *Commun. Chem.* **5** 7
[5] Gentile P, Cuoco M, Volkov O M, Ying Z J, Vera-Marun I J, Makarov D and Ortix C 2022 *Nat. Electron.* **5** 551
[6] Schultheiss V H, Batz S and Peschel U 2016 *Nat. Photon.* **10** 106
[7] Bekenstein R, Kabessa Y, Sharabi Y, *et al.* 2017 *Nat. Photon.* **11** 664
[8] Schultheiss V H, Batz S, Szameit A, Dreisow F, Nolte S, Tünnermann A, Longhi S and Peschel U 2010 *Phys. Rev. Lett.* **105** 143901
[9] Carollo R A, Aveline D C, Rhyno B, Vishveshwara S, Lannert C, Murphree J D, Elliott E R, Williams J R, Thompson R J and Lundblad N 2022 *Nature* **606** 281
[10] Jia F, Huang Z, Qiu L, Zhou R, Yan Y and Wang D 2022 *Phys. Rev. Lett.* **129** 243402
[11] Jensen H and Koppe H 1971 *Ann. Phys.* **63** 586
[12] da Costa R C T 1981 *Phys. Rev. A* **23** 1982
[13] Szameit A, Dreisow F, Heinrich M, Keil R, Nolte S, Tünnermann A and Longhi S 2010 *Phys. Rev. Lett.* **104** 150403
[14] Cantele G, Ninno D and Iadonisi G 2000 *J. Phys.: Condens. Matter* **12** 9019
[15] Silva K V R A, de Freitas C F and Filgueiras C 2013 *Eur. Phys. J. B* **86** 147
[16] Longhi S 2007 *Opt. Lett.* **32** 2647
[17] Spittel R, Uebel P, Bartelt H and Schmidt M A 2015 *Opt. Express* **23** 12174
[18] Stockhofe J and Schmelcher P 2014 *Phys. Rev. A* **89** 033630
[19] Ferrari G and Cuoghi G 2008 *Phys. Rev. Lett.* **100** 230403
[20] Brandt F T and S'anchez-Monroy J A 2015 *Europhys. Lett.* **111** 67004
[21] Wang Y L and Zong H S 2016 *Ann. Phys.* **364** 68
[22] Ouyang P, Mohta V and Jaffe R 1999 *Ann. Phys.* **275** 297
[23] Burgess M and Jensen B 1993 *Phys. Rev. A* **48** 1861
[24] Brandt F T and Sánchez-Monroy J A 2016 *Phys. Lett. A* **380** 3036
[25] Ortix C 2015 *Phys. Rev. B* **91** 245412
[26] Entin M V and Magarill L I 2001 *Phys. Rev. B* **64** 085330
[27] Chang J Y, Wu J S and Chang C R 2013 *Phys. Rev. B* **87** 174413
[28] Wang Y L, Du L, Xu C T, Liu X J and Zong H S 2014 *Phys. Rev. A* **90** 042117
[29] Wang Y L, Jiang H and Zong H S 2017 *Phys. Rev. A* **96** 022116
[30] Liang G H, Wang Y L, Lai M Y, Liu H, Zong H S and Zhu S N 2018 *Phys. Rev. A* **98** 062112
[31] Maraner P and Destri C 1993 *Mod. Phys. Lett. A* **08** 861
[32] Maraner P 1995 *J. Phys. A: Math. Gen.* **28** 2939
[33] Maraner P 1996 *Ann. Phys.* **246** 325
[34] Fujii K, Ogawa N, Uchiyama S and Chepilko N M 1997 *Int. J. Mod. Phys. A* **12** 5235
[35] Schuster P and Jaffe R 2003 *Ann. Phys.* **307** 132
[36] Meschede L, Schwager B, Schulz D and Berakdar J 2023 *Phys. Rev. A* **107** 062806
[37] Batz S and Peschel U 2008 *Phys. Rev. A* **78** 043821
[38] Lai M Y, Wang Y L, Liang G H, Wang F and Zong H S 2018 *Phys. Rev. A* **97** 033843
[39] Lai M Y, Wang Y L, Liang G H and Zong H S 2019 *Phys. Rev. A* **100** 033825
[40] Gaididei Y, Kravchuk V P and Sheka D D 2014 *Phys. Rev. Lett.* **112** 257203
[41] Streubel R, Fischer P, Kronast F, Kravchuk V P, Sheka D D, Gaididei Y, Schmidt O G and Makarov D 2016 *J. Phys. D: Appl. Phys.* **49** 363001
[42] Caracanhas M A, Massignan P and Fetter A L 2022 *Phys. Rev. A* **105** 023307
[43] Salasnich L 2022 *SciPost Phys. Core* **5** 015
[44] Liang G H and Lai M Y 2023 *Phys. Rev. A* **107** 022213
[45] Hooft G 2005 *50 years of Yang–Mills theory* (Singapore: World Scientific)